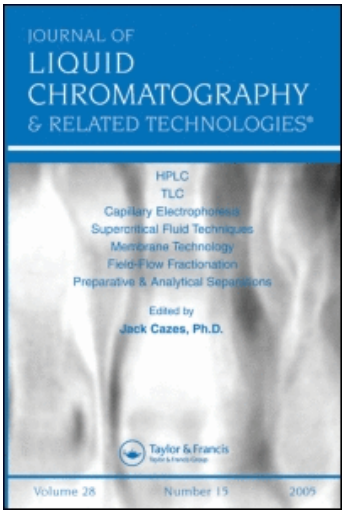

Journal of Liquid Chromatography & Related Technologies
Publication details, including instructions for authors and subscription information:
http://www.informaworld.com/smpp/title~content=t713597273

Characterization and High Performance Liquid Chromatographic Evaluation of a New Amide-Functionalized Reversed Phase Column

Tracy L. Ascah[a]; Krishna M. R. Kallury[a]; Cory A. Szafranski[a]; Scott D. Corman[a]; Francis Liu[a]
[a] Supelco, Inc. Supelco Park,

To cite this Article Ascah, Tracy L. , Kallury, Krishna M. R. , Szafranski, Cory A. , Corman, Scott D. and Liu, Francis(1996) 'Characterization and High Performance Liquid Chromatographic Evaluation of a New Amide-Functionalized Reversed Phase Column', Journal of Liquid Chromatography & Related Technologies, 19: 17, 3049 — 3073
To link to this Article: DOI: 10.1080/10826079608015125
URL: http://dx.doi.org/10.1080/10826079608015125

J. LIQ. CHROM. & REL. TECHNOL., 19(17&18), 3049–3073 (1996)

CHARACTERIZATION AND HIGH PERFORMANCE LIQUID CHROMATOGRAPHIC EVALUATION OF A NEW AMIDE-FUNCTIONALIZED REVERSED PHASE COLUMN

Tracy L. Ascah, Krishna M. R. Kallury, Cory A. Szafranski, Scott D. Corman, Francis Liu

Supelco, Inc.
Supelco Park
Bellefonte, Pennsylvania 16823

ABSTRACT

A new amide-functionalized silica stationary phase, Supelcosil ABZ$^+$ Plus, suitable for reversed phase HPLC applications, was characterized by X-ray photoelectron spectroscopy (XPS), solid-state ^{29}Si and ^{13}C CP/MAS NMR and FTIR. The degree of hydration of this material was found to be much higher compared to amide-functionalized silica phases prepared by acid chloride treatment of aminopropylsilylated silica reported earlier and also compared to conventional C_{18} reversed phase columns. The liquid chromatographic performance of this ABZ$^+$ Plus column was found to be superior to the C_{18} columns, especially for polar analytes. The enhanced selectivity and better peak shape with this ABZ$^+$ Plus material was attributed to greater compositional differences between the surface and mobile phases coupled with more effective shielding of residual silanols and a more oriented alkyl chain structure.

INTRODUCTION

High performance liquid chromatography is an invaluable analytical tool that finds application in diverse areas which deal with the isolation, production and distribution of chemicals. Examples of such fields include environmental monitoring/control,[1] drugs/pharmaceutical production,[2] generation/purification of blood or plasma products,[3] biotechnological advances such as recombinant DNA-based proteins and other biochemicals[4,5] and food products,[6,7] to name a few. Silica-based C_8 and C_{18} columns are the most extensively used analytical probes for a vast majority of these applications.[8] Selection of a column most appropriate for a particular type of application depends upon the nature of the analyte(s). Thus, for the analysis of non-polar analytes such as small aromatic hydrocarbons, the choice is presumed to be the least complicated (although recent reviews[9-13] prove that even this is no trivial matter). However, the situation becomes extremely complex when analytes are polar or moderately polar small organic molecules with basic or acidic substituents, such as pharmaceuticals. Large differences are encountered by analysts dealing with such molecules, with respect to retention, selectivity and peak shape, even with ostensibly equivalent columns packed with C_{18} materials.[14]

Incomplete reaction of the silica surface silanols with a silanizing reagent or the formation of new silanols, when bi- or tri-functional modifiers are utilized, is a problem that continues to plague the area of liquid chromatography employing bonded phases, since these functionalities affect both retention and peak shape. Partial solutions for this problem consist of end-capping,[15] addition of organic modifiers to the mobile phase,[16] introduction of bulkier substituents on the silicon atom of the silane reagent in place of the methyl groups,[17-19] use of bidentate ligands,[20] formation of Si_{silica}-$C_{alkyl\ chain}$ bond in place of the normal siloxane bond between the silica and silane silicon atoms[21] and the use of mixed trifunctional silanes.[22] Nevertheless, the deliterious effect of surface silanols has not been resolved to the satisfaction of practising chromatographers.

A totally different approach towards minimizing the effect of residual silanols is to generate a functionality on the modified silica surface that can react with the silica silanols through electrostatic and/or hydrogen-bonding interactions. Of particular interest is the amide group which possesses attractive properties such as stability to bases, strong H-bond forming capabilities and non-reactivity with different chemical functionalities present on small polar organic molecules. The most convenient method of introducing the amide moiety is through the acylation of a pre-formed aminopropylsilylated silica surface. Tundo and Venturello[23] have adopted this approach as far back as 1979 to prepare silica-based phase transfer catalysts carrying the

acylaminoalkyl chain. An analogous surface modification procedure has been utilized by Oi and coworkers[24] in 1983 to prepare an acylaminoalkylsilylated silica stationary phase suitable for chiral liquid chromatography. Nomura and coworkers[25] subsequently investigated the acylation of aminopropylsilica with a variety of acid chlorides. This study was followed by the work of Buszewski and coworkers[26] with extensive solid-state NMR and chromatographic studies on similar acylamino-derivatized silicas, termed "peptide bond carrying silicas" by the authors. Similar amide-functionalized silicas were reported by Okahata et al.,[27] Boven et al.,[28] Yamamura et al.,[29] Pidgeon et al.,[30] Kallury et al.,[31] Ihara et al.,[32] Nagae et al.,[33] the Pirkle group[34] and by Meyerhoff and coworkers,[35] which were utilized for a variety of analytical and synthetic applications, besides liquid chromatography. An analogous functionalized silica surface carrying urethane functionalities instead of amide moieties has also been reported recently.[36]

The above brief summary reveals that although amide-functionalized silica phases have been synthesized and used for a wide range of applications, surface coverage data, the nature of interactions between the amide moiety and the surface silanols of the silica and retention mechanism studies have been scarce. The only reported surface coverage evaluations appear to be those from the Meyerhoff group dealing with a carboxytetraphenylporphyrin bound to aminopropylsilylated silica[35] and the Buszewski group on amide-functionalized silica surfaces prepared by a two-step procedure,[37] based on elemental analysis. In the current paper, X-ray photoelectron spectroscopy in combination with FTIR and ^{13}C and ^{29}Si CP/MAS NMR was utilized to probe the surface structure of Supelcosil ABZ$^+$ Plus, a new amide-functionalized silica stationary phase, and the surface characteristics of ABZ$^+$ Plus were compared with those of its precursor, ABZ, and a conventional C_{18} reversed phase silica. The chromatographic performance of this new amide-derivatized silica stationary phase ABZ$^+$ Plus was evaluated in the present work employing a wide selection of organic molecules widely differing in their polarities and it was demonstrated that this new LC column is superior to the conventional C_{18} reversed phase columns.

The chromatographic applications of Supelcosil ABZ, the other amide-functionalized stationary phase have been elaborated in several recent publications[38-41] and will not be discussed in the current work. The ABZ$^+$ Plus material was made by a single step surface attachment procedure, while the ABZ phase was made by a two-step protocol. The residual amino moieties on the ABZ phase were acetylated after the introduction of the longer acyl chain. The ABZ and ABZ$^+$ Plus materials contain the same number of carbon atoms in their alkyl chains as the C_{18} material.

EXPERIMENTAL

Materials

The analytes included in the present study were procured from either Aldrich or Sigma and were used as such. The solvents utilized were all HPLC grade and obtained from Baker. The chromatographic columns Supelcosil ABZ$^+$ Plus. ABZ and LC-18DB were supplied by Supelco, Inc., Bellefonte, PA. The amide-functionalized stationary phase materials were generated from high purity silica with a surface area of 330 m^2/g and a pore volume of 0.6 cm^3/g.

Spectroscopic Analysis

The solid state ^{29}Si CP/MAS NMR spectra were recorded on a modified NT-270 Nicolet NMR spectrometer. Spectra were obtained in natural abundance at a frequency of 53.76 MHz employing a contact time of 10ms, high power proton decoupling during acquisition, a recycle delay of 3 sec and a spectral width of 20 kHz. MAS was carried out at 4.0 kHz. Cross-polarization (CP) and magic angle spinning (MAS) were performed using a multinuclear CP/MAS probe equipped to accommodate 7.0 mm spinners.

Typically, 4500 transients were accumulated. The ^{13}C CP/MAS NMR spectra were collected at 68.055 MHz with a contact time of 5 ms and MAS was carried out at 4.2 kHz. Typically, 3000 transients were collected for these spectra.

X-ray photoelectron spectra were recorded on a Kratos XSAM 800PCI using an unmonochromated Mg K_α source run at 14 kV and 20 mA. The samples were mounted on a gold-coated cup. The shape of the spectra indicated that no compensation for differential surface charging was needed. The binding energy scale was calibrated to 285.0 eV for the main C(1s) C-C feature. Spectra were run in both low resolution and high resolution modes (pass energy 40 eV) for the C(1s), N(1s), Si(2p) and O(1s) regions. Each sample was analysed at a 75° angle relative to the electron detector. An analysis area of 3 mm was used for rapid data collection.

Elemental compositions were calculated from the high resolution spectra normalized for constant transmission using the software supplied by the manufacturer. ATR-FTIR spectra were recorded on a Mattson 2020 infrared spectrometer in potassium bromide.

Table 1

X-Ray Photoelectron Spectroscopic Data on ABZ, ABZ$^+$ Plus and C_{18} Silicas

	Elemental Composition (%)				High Resolution Data			
					C(1s)		N (1s)	
	C (ls)	Si (2p)	O (ls)	N (1s)	Binding Energy (eV)	Area (%)	Binding Energy (eV)	Area (%)
ABZ	43.1	22.3	32.4	2.2	285.0	94	399.7	69.9
					287.4	6	401.0	24.3
							402.9	6.8
ABZ$^+$ Plus	42.5	22.2	33.1	2.2	285.0	94	399.6	63.1
					287.0	6	400.6	28.1
							402.3	8.8
C_{18}	44.4	24.0	31.6	---	285.0	100	No nitrogen present	

Apparatus

The analytical system consisted of a HP 1090 Liquid Chromatograph, with UV detection at 254 nm and a flow rate of 2.0 mL/min. The mobile phase was 10mM potassium dihydrogen phosphate containing acetonitrile (70:30 or 60:40). Peaks were integrated by a HP3396 Series II integrator.

RESULTS AND DISCUSSION

Characterization of the Standard C_{18}, ABZ and ABZ$^+$ Plus Stationary Phases

The surface analytical techniques most extensively used for characterizing particulate materials are FTIR, solid-state CP/MAS NMR and X-ray photoelectron spectroscopy (XPS, also known as electron spectroscopy for chemical analysis, ESCA)[42]. The former two are invaluable in functional group analysis and in the evaluation of the motional dynamics of the alkyl chains on

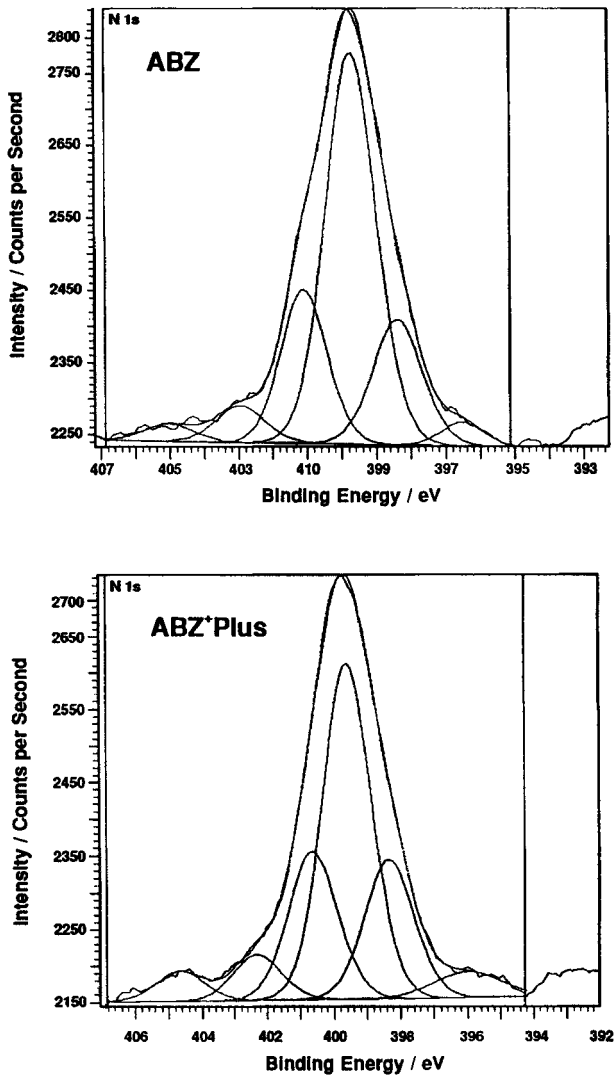

Figure 1. X-ray photoelectron spectra of Supelcosil ABZ and ABZ$^+$ Plus amide-functionalized silicas: N(1s) binding energy region.

the silane silicon of the surface-treated silicas. XPS, on the other hand, is unique since it provides quantitative structural and functional group information from sub-monolayer level surface coverages to multi-layers up to a thickness of 10 nm, in addition to elemental composition data.

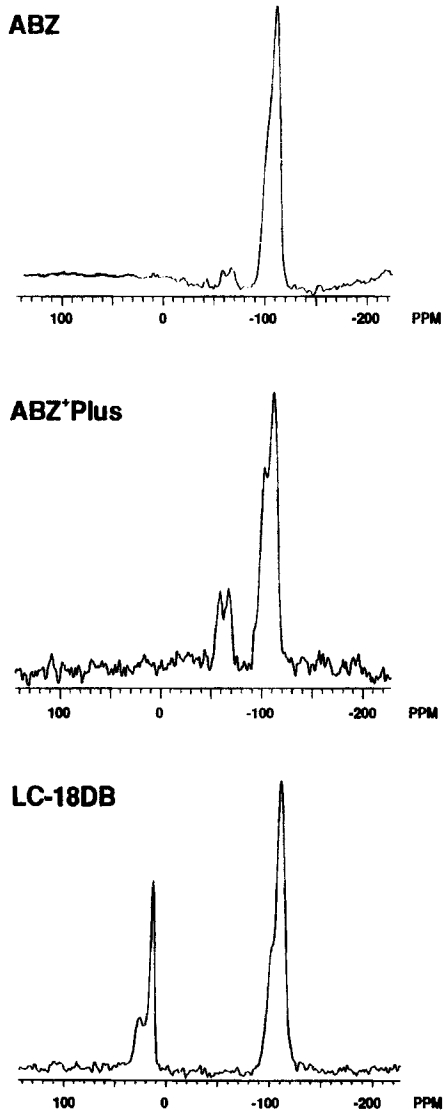

Figure 2. Solid-state ^{29}Si CP/MAS NMR spectra of Supelcosil ABZ, ABZ^{+} Plus and LC-18DB silicas.

Consequently, XPS is a surface analysis tool as opposed to FTIR and NMR which are bulk analytical probes. The XP spectra of ABZ and ABZ$^+$ Plus silica are included in Figure 1 and the elemental compositions of the two surfaces given in Table 1. Based on the carbon percentage derived from XPS data, surface coverage of an organic layer in general and of silane-modified silicas in particular can be calculated by Equation 1.[43]

$$\Gamma_{sox} = [10^6/S_{BET}]\,[(1201a_c/P_c) - M(Su) + \delta]^{-1} \qquad (1)$$

where, Γ_{sox}=surface concentration of the organic species on the silica surface in μmol/m^2; S_{BET}=specific surface area of untreated silica, a_c=number of carbon atoms on the organic species attached to the surface, P_c=percent of carbon on the modified silica surface, M(Su)=molecular weight of the silyl unit on the silica surface and δ=correction factor for desorbed water (usually taken as 5).

From Equation 1, the surface coverages of the ABZ$^+$ Plus, ABZ and standard non-functional C_{18} silica could be calculated by substituting the values of carbon percentage P_c derived either from elemental analyses or from the XPS data. Employing the carbon percentages of 12.87, 12.01 and 11.87 for ABZ$^+$ Plus, ABZ and C_{18}, respectively, obtained by elemental analyses, the surface coverages work out to 2.35, 2.15 and 2.12 μmol/m^2 for these three surfaces in that order. On the other hand, utilizing the atom percent values derived from the C(1s) binding energy peaks recorded in the XP spectra, the same surface coverages were computed as 14.86, 13.90 and 14.60 μmol/m^2, respectively. For computing the surface coverage of the non-functional monomeric C_{18} silica, data from earlier literature (44,45) was utilized. It is obvious that the surface coverage values obtained from the XPS data are about seven times greater than those measured from the elemental analysis data (and the carbon percentage values are 3-4 times greater for the XPS method compared to elemental analyses).

A similar discrepancy has been reported by Brown and coworkers,[46] who studied monomeric alkyl bonded phases by XPS and SIMS techniques. Their results show that the XPS-derived carbon percentages are higher by a factor of 2-3 than those obtained from elemental analysis. In our current study, the amide-functionalized silica surfaces are polymeric in nature and hence cross-linking is to be expected. If the XPS-derived carbon percentages are any indication, our polymeric surfaces contain nearly twice as much carbon as the monomeric C_{18} reported by Brown et al.[46] However, the elemental analysis data shows that the carbon percentages of our polymeric C_{18} surface (11.87) and their monomeric C_{18} surface (10.64) are not that different. Furthermore, Buszewski and coworkers[47] report that the carbon percentages obtained from

elemental analyses are 4.93 for monomeric aminopropyl bonded phase and 4.66 for polymeric aminopropyl bonded phase; for the corresponding AA_6 phases obtained by acylation with hexanolyl chloride, the carbon values are 9.93 and 9.47, respectively.

Our XPS results on the same monomeric and polymeric aminopropylsilylated silicas indicate that the carbon content of the latter is about twice that of the former.[48] FTIR spectroscopic data on all of the silica surfaces cited above support the fact that the carbon content of polymeric materials is much higher than the corresponding monomeric materials,[49] in spite of the fact that there are two additional methyl carbons on the silicon of the latter. It is thus clear that elemental analysis does not distinguish clearly between monomeric and polymeric alkylsilylated stationary phases with respect to their carbon contents. On the other hand, the XPS technique is more reliable since it probes only the top 5-10 nm of a surface with minimal interference from the bulk silica layers underneath and reflects the surface composition more accurately. Owing to the limited depth probing capability of the X-ray beam in XPS, the entire silane layer is scanned together with the silica underneath this layer to a depth of 3-4 nm. Therefore, the carbon content (and hence the surface coverage of the silane) appears to be higher than the silanol content which is computed to be around 8 $\mu mol/m^2$. Since the chromatographic properties of bonded phases are dependent primarily on the surface structure rather than the bulk structure of silica, it is reasonable to assume that XPS provides a more accurate measure of the chromatographic performance of a modified silica stationary phase than elemental analysis. From the XPS results registered in the current work, as well as those reported by others earlier, it is evident that about 90% of the total bound silane is present at the silica surface.

Both elemental composition and XPS data on the ABZ^+ Plus, ABZ and C_{18} surfaces indicate that there is no significant difference between the three types of silica (C_{18}, ABZ and ABZ^+ Plus) with respect to their surface coverages. However, both ABZ and ABZ^+ Plus carry the amide functionalities and obviously, there are bound to be differences in the nature of interactions these two surfaces exhibit with silica silanols as opposed to the non-functional C_{18} silicas. The non-functional C_{18} silica is hydrophobic (since it contains only the octadecyl chain and no other functionality) and shows only one C(1s) binding energy peak in its XPS at 285.0 eV which is assignable to the carbon atoms of the C_{18} alkyl chain. The amide-containing silicas exhibit two C(1s) binding energy peaks, at 285.0 and 287.2±0.2 eV, representing the hydrocarbon and amide carbons, respectively, in a 10:1 ratio (the theoretical value for this ratio is 9:1).

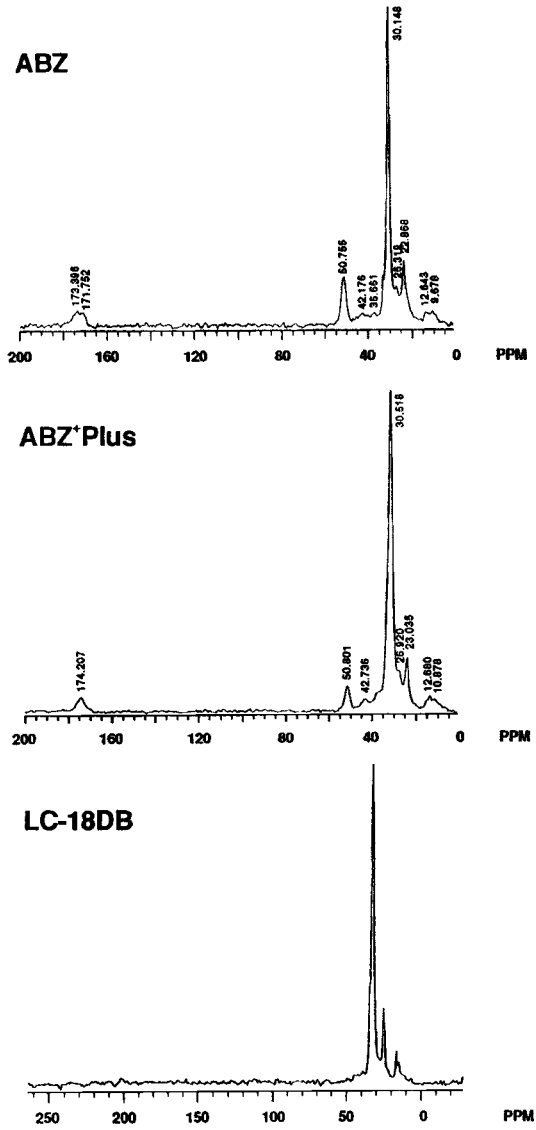

Figure 3. Solid-state ^{13}C CP/MAS NMR spectra of Supelcosil ABZ, ABZ^{+} Plus and LC-18DB silicas.

The N(1s) binding energy region (see Figure 1 and Table 1) throws significant light into the nature of interactions of the amide moiety in ABZ and ABZ$^+$ Plus with silica surface silanols. With both silicas, six peaks were registered in this region; however, two of them , which occur at the extremes of the binding energy scale, are due to charging and were not taken into account (these two account for only 5-6% of the total nitrogen). Two of the remaining four peaks were observed at approximately the same binding energy values, viz. 398.37±0.01 eV and 399.65±0.04 eV, respectively; with both silicas. The former is attributable to a more negative nitrogen atom resulting from strong H-bonding between the NH of the amide (to which this nitrogen belongs) and the carbonyl group of an adjacent amide moiety. The latter represents the non-hydrogen-bonded component of the amide functionality and is more prevalent with ABZ compared to ABZ$^+$ Plus. In addition, two other peaks were recorded for both silicas in the N(1s) binding energy region, at 400.8±0.2 and 402.6±0.3 eV, respectively. These two peaks form 24% of the total nitrogen with ABZ and 30% with ABZ$^+$ Plus silicas and represent the H-bonded fractions of the total amide moieties in either case.

Significantly, there is a 0.4 eV and 0.6 eV binding energy difference between the ABZ and ABZ$^+$ Plus amide functions with respect to the 400.8±0.2 and 402.6±0.3 eV peaks, respectively, indicating that the amide functionality in ABZ is more strongly hydrogen-bonded than in ABZ$^+$ Plus. This discrepancy is attributable to the variation in the moieties involved in H-bonding with the amide functionality on the two silica surfaces. Thus, in ABZ the amide groups appear to be H-bonded to the silica/silane silanols and in ABZ$^+$ Plus, they are H-bonded to water. This hypothesis derives strong support from the solid-state ^{29}Si CP/MAS spectra of the two amide-functionalized silicas (see Figure 2 for the spectra). The Q_3, T_3 and T_4 type[50] of ^{29}Si peaks for ABZ are shifted about 1.1 ppm downfield compared to the corresponding peaks in ABZ$^+$ Plus. The Q_3 peak in the ^{29}Si NMR spectrum of ABZ$^+$ Plus appears around the same frequency as for LC-18DB pointing to the same type of environment for this silica silicon atom in both samples; the LC-18DB sample contains an additional peak for the M_1 type of silicon (attached to two methyl groups and the C_{18} alkyl chain, with a single attachment to the silica surface) in its ^{29}Si NMR spectrum. However, there seems to be a significant difference in the degree of hydration of the ABZ$^+$ Plus and the LC-18DB silica surfaces, as evidenced by the higher oxygen content (about 4%) in the XPS of the former in comparison with the O(1s) peak intensity of the latter. It is to be noted that the Si(2p) binding energy peak intensities of ABZ$^+$ Plus and LC-18DB are about the same and the surface coverages are also roughly equal in the two samples. It is this water layer that contributes to the better chromatographic performance of the ABZ$^+$ Plus material than that observed with standard C_{18} reversed phase columns, as discussed in the next section.

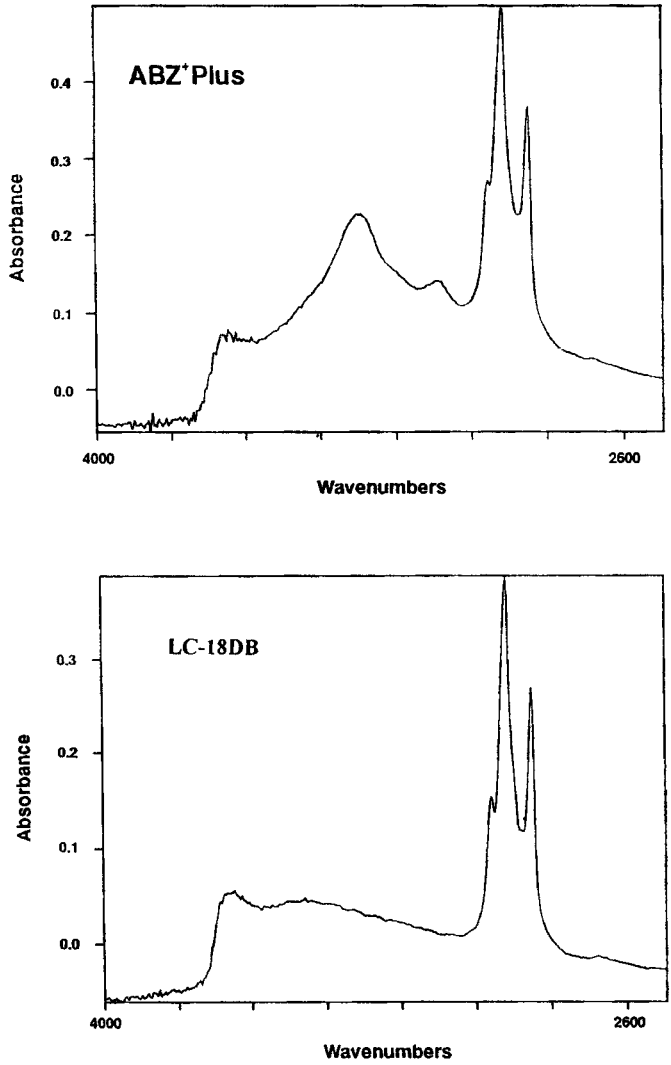

Figure 4. FTIR spectra of Supelcosil ABZ$^+$ Plus and LC-18DB silicas.

Further confirmation of the difference in the H-bonding strengths of ABZ and ABZ$^+$ Plus is obtained from the ^{13}C CP/MAS NMR spectra of the two surfaces (see Figure 3). The carbon β- to the silicon atom of the silane appears at 26.318 ppm with ABZ, while the same carbon in ABZ$^+$ Plus is registered at 26.920 ppm.

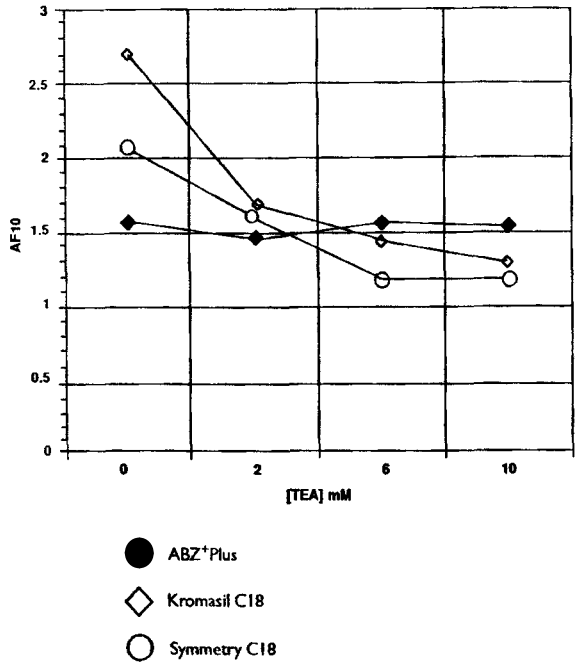

Figure 5. Asymmetry factor of the codeine peak as a function of triethylamine concentration for Supelcosil ABZ$^+$ Plus, Kromasil C-18 and Symmetry C$_{18}$ columns.

It has been established earlier[51] that the β-carbon in aminopropylsilylated silica shifts from around 27 ppm to around 22 ppm upon hydration of the surface. In this instance, the mechanism proposed involves the protonation of the amino nitrogen with a proton from the silica surface silanol and stabilization of the charged species by the surface water. In the current context, the silane functionality in ABZ is the amide instead of the amine and the proton abstraction occurs through the carbonyl group of the amide with consequent stabilization by the surface water. Hence, the β-carbon in ABZ is upfield shifted in comparison with ABZ$^+$ Plus surface.

It is difficult to derive quantitative information from the ATR-FTIR spectra of the ABZ$^+$ Plus and ABZ surfaces (see Figure 4 for the FTIR spectrum of the former), but a clear distinction between ABZ$^+$ Plus and LC-18DB could be noticed both in the amide carbonyl region and the OH stretching region reflecting the structural differences between these two silica surfaces.

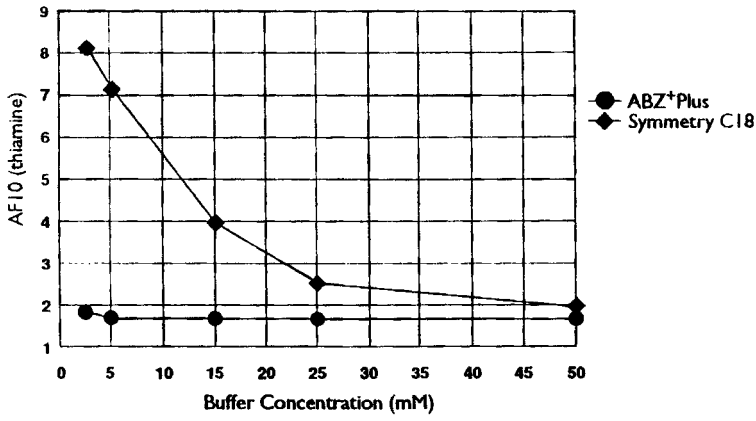

Figure 6. AF_{10} (thiamine) as a function of buffer concentration for Supelcosil ABZ^+ Plus and Symmetry C_{18} columns.

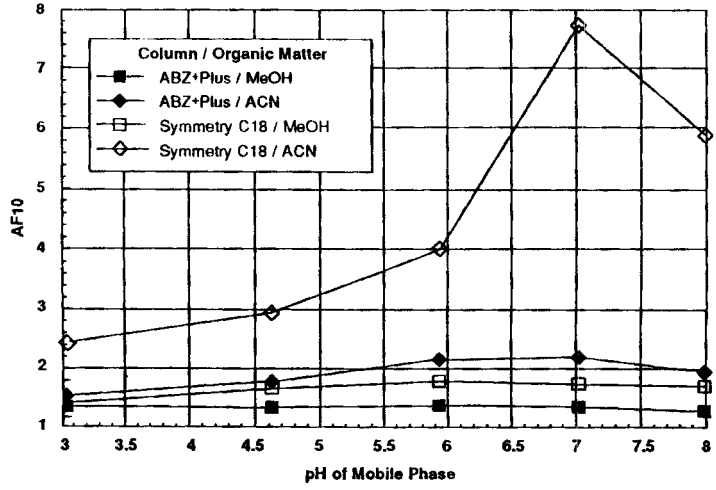

Figure 7. Effect of variation of mobile phase pH on peak shape of amytriptyline (without amine modifier) for Supelcosil ABZ^+ Plus and Symmetry C_{18} columns.

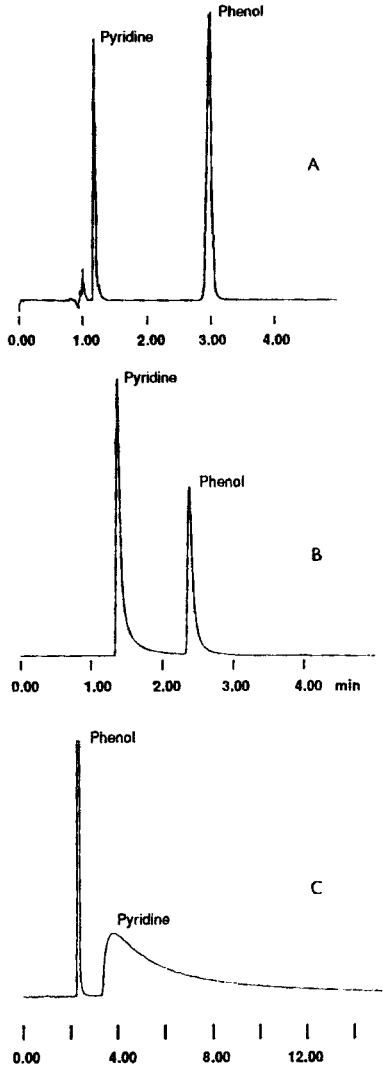

Figure 8. Comparison of the deactivation levels of Supelcosil ABZ$^+$ Plus, LC-18DB and LC-18 columns for mixtures of phenol and pyridine.

Table 2

Comparison of Deactivated Columns for Chromatography and Resolution of Acids

Column	K'_{Sorbic}	$K'_{Benzoic}$	N_{sorbic} (Plates/m)	$N_{benzoic}$ (Plates/m)	AF_{10} Sorbic	AF_{10} Benzoic	Res
Supelcosil ABZ+Plus[a]	4.3	5.1	68,300	67,800	1.3	1.4	3.5
YMC-Basic[a]	2.2	2.4	68,200	69, 300	1.2	1.4	0.9
LiChrosorb RP-Select B[b]	3.2	3.6	49,200	37,900	2.7	3.7	2.6
Intersil ODS-2[a]	2.6	2.7	50,500	50,400	1.2	1.3	0.8
Hypersil BDS-C18[a]	2.9	3.0	74,700	87,900	1.5	1.6	0.3
TSKgel ODS-80Ts[a]	2.8	3.0	109,600	110,900	1.2	1.2	1.5
Nucleosil 100-5 C18 AB[c]	2.6	2.7	53,900	60,000	2.2	2.0	0.4
Zorbax R_x[b]	3.8	4.2	82,900	94,300	1.3	1.3	2.6
Waters Symmetry C_8[a]	5.3	5.3	47,900	33,600	5.6	7.4	0.0
Waters Symmetry C_{18}[a]	4.9	5.0	62,900	60,900	2.0	2.2	0.5

Mobile Phase: acetonitrile: 25mM KH_2PO_4 (pH 7.0), 25:75
Flow Rate: 1mL/min
[a] 15cm column
[b] 25cm column
[c] 10cm column

Comparison of the Liquid Chromatographic Behaviour of the ABZ$^+$ Plus and the C_{18} Reversed Phase Columns

The inherent level of deactivation of the ABZ$^+$ Plus stationary phase with respect to the conventional reversed phase C_{18} materials, when analytes such as codeine, thiamine or amitryptiline are subjected to liquid chromatographic analysis, is illustrated in Figures 5-7. In Figure 5, the asymmetry factor of the codeine peak at different concentrations of triethylamine was used as an index to assess the residual silanol effects. In all these experiments, the pH of the mobile phase was maintained at 7.0 so that the silanols are not protonated and their influence on the analyte elution profile could be more clearly visualized.

It is evident from Figure 5 that both types of C_{18} columns investigated show marked improvement in peak shape upon the addition of triethylamine, whereas this base additive had no influence on the codeine peak shape whatsoever with the ABZ$^+$ Plus column. Similarly, Figure 6 shows that ionic strength had no effect on the peak shape of thiamine when analysed on the ABZ$^+$ Plus column, while it exerts a significant effect on the peak shape with the C_{18} column.

Figure 7 demonstrates the influence of changing the mobile phase composition on the peak shape of amitryptiline in the absence of an amine modifier. In both acetonitrile and methanol, the peak shape on the ABZ$^+$ Plus column is good; however, with pure-silica C_{18} the peak shape is poor at pH 7.0 indicating the influence of reactive silanol sites on this silica.

Figure 8 demonstrates the difference between a standard C_{18}, a conventional deactivated C_{18} and the ABZ$^+$ Plus columns when a mixture of pyridine and phenol is eluted under identical conditions. Again, the best results are obtained with the ABZ$^+$ Plus column which shows that both the acidic and basic silanol sites are shielded in this column. Table 2 shows the values of k', N and AF obtained for ten different columns with codeine under identical elution conditions. The data clearly indicate that Supelcosil ABZ$^+$ Plus is the best column with respect to peak shape.

The selectivity achievable with the ABZ$^+$ Plus column is illustrated in Figure 9 for a mixture of three basic drugs and for a mixture of acids, in comparison with Symmetry C_{18} column. The former were eluted at pH 7.0 and the latter at pH 2.3.

The superiority of the ABZ$^+$ Plus columns over conventional C_{18} columns with respect to selectivity is readily recognized from the series of alkyl-benzenes, -anilines and -benzoic acids indicated in Figure 10. The retention

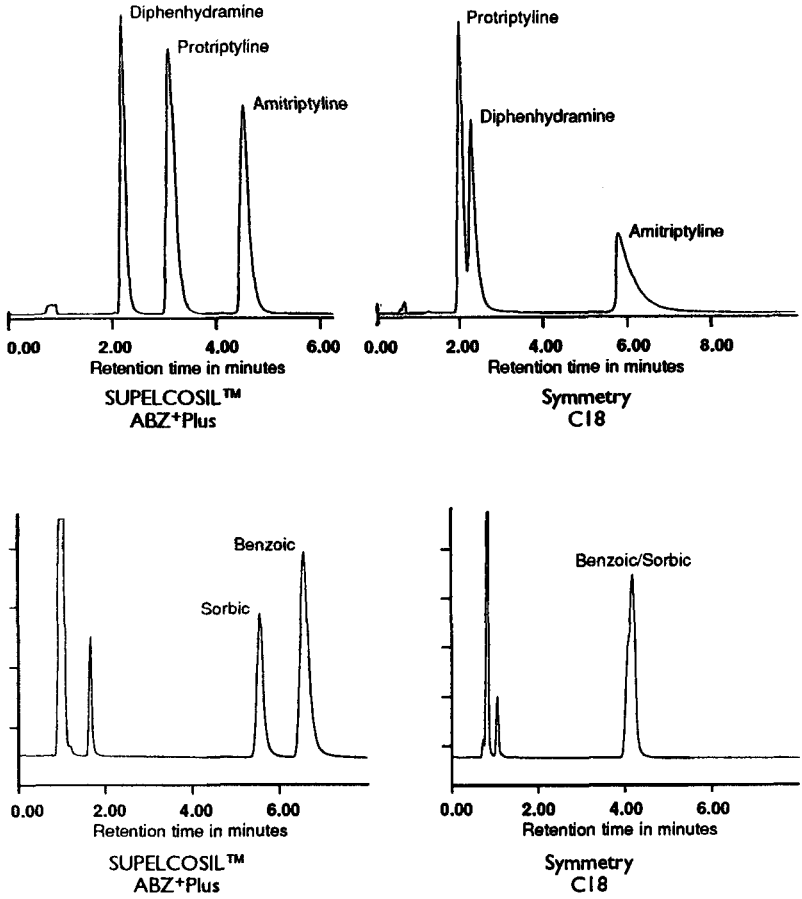

Figure 9. Comparison of the selectivities for three basic drugs and a mixture of sorbic and benzoic acids on Supelcosil ABZ$^+$ Plus and Symmetry C_{18} columns.

times for alkylbenzenes and anilines were shorter with the ABZ$^+$ Plus column, while the acids were retained longer as compared to the C_{18} column. This data clearly shows that the ABZ$^+$ Plus material is more polar than the C_{18} stationary phase.

As indicated in the characterization section, the difference between ABZ$^+$ Plus and a conventional C_{18} column is that in the former there is an amide group close to the silica surface coupled with the fact that there is a significant hydration layer at the surface. The ABZ$^+$ Plus organic surface layer is

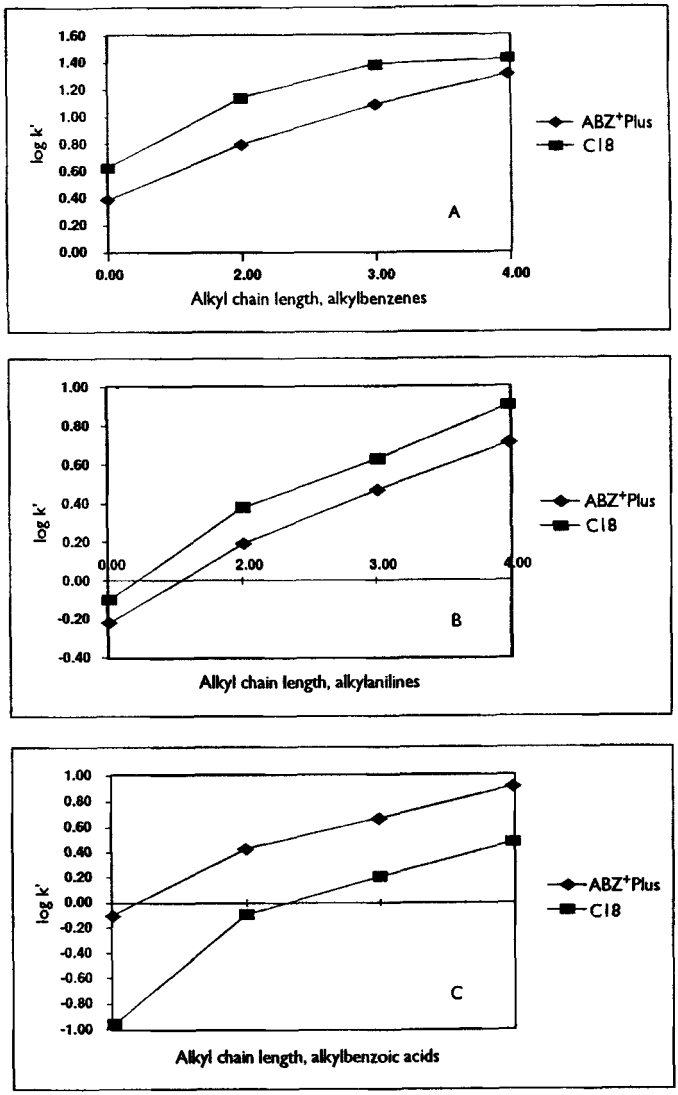

Figure 10. Selectivities of Superlcosil ABZ$^+$ Plus and C_{18} columns for alkyl-benzenes, -anilines and -benzoic acids.

amphiphilic with a polar functionality at the silica surface and a long alkyl chain extending into the stationary phase-mobile phase interface. This structural feature is analogous to a lipid membrane in a biological system which is known to be hydrated at the polar head group region.[52] Such surface-

immobilized structures were shown to interact with a variety of functionalized organic molecules through a partition mechanism, making use of electrochemical methods of analysis.[53] Similar partitioning mechanisms were proposed by Martire[54] and by Dill[55] through a unified molecular theory based on a lattice model and statistical-mechanical theory that takes into account bonded-chain reorganization energy, respectively, for solute retention on monomeric C_{18} bonded reversed phases.

Marshall and coworkers[56] have estimated through fluorescence measurements employing dansyl probes that the interfacial region of RP-18 stationary phase has an effective polarity comparable to that of methanol containing 10% water. It is presumed that the organic modifier in mixed organic-water mobile phases is preferentially adsorbed at this interface and thus the solvent composition of the stationary phase zone is different from that of the mobile phase varying with the distance from the silica surface. Partitioning of the solute takes place between the mobile phase and this zone and is dependent upon its polarity and dimensions.

Jaroniec[57] has recently pointed out that the composition of the solvents in the stationary phase significantly influences the solute's retention even in the the case of conventional bonded phases and that this effect is much stronger for silica-based packings with chemically bonded phases of specific properties. It has been demonstrated that the stationary phase plays a vital role in liquid chromatographic separations in RPLC in general and when the bonded reversed phase contains ligands carrying amide functionalities, in particular.[58-60] The factors that govern the thermodynamic equilibrium of solvent distribution between the mobile and stationary phases include the mobile phase composition, the chemical nature of the bonded ligands, their surface concentration and conformation. Furthermore, the hydrogen bonding interactions associated with the residual silanols on the modified silica also play a significant role in controlling the concentration of water molecules in the chemically bonded phase and consequently exert a profound effect on the composition of this phase. The pioneering work of the Jaroniec group[58-63] on the measurement of sorption excessess at the liquid-solid interface when aqueous-organic binary mobile phase systems are used in HPLC sheds considerable light on the liquid chromatographic behaviour of amide-functionalized stationary phases. Of particular interest is the observation that the sorption excess of water for the C_{18} and AA_3 (octadecanoylaminopropyl-silanized silica) reversed phases are similar and negative, while that for AA_2 (a shorter chain analogue of AA_3) it is positive. Both AA_3 and AA_2 exhibit good symmetry and peak shapes for polar molecules, especially basic compounds.

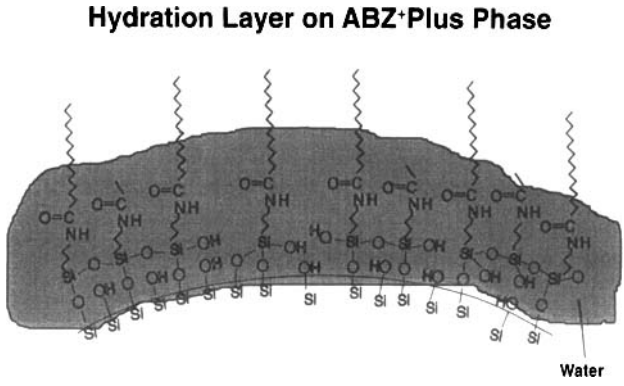

Figure 11. Structure of Supelcosil ABZ$^+$ Plus stationary phase with its hydration layer.

With the current ABZ$^+$ Plus material, we hypothesize that the combination of the surface amide functionalities and the larger hydration layer at the silica surface imparts a high degree of orientation to the alkyl chains of this stationary phase. When this phase is contacted by the binary water-acetonitrile mobile phase, the ensuing equilibration results in a profound difference between the solvent compositions of the stationary and mobile phases, which contributes to a more effective partitioning of a polar solute and results in greater selectivity. Moreover, the large hydration layer can also shield the residual silanols of the silica from the solute (see Figure 11) more effectively.

In contrast to the high degree of orientation of the ABZ$^+$ Plus material, the alkyl chains on the conventional C_{18} reversed phase columns can fold back and block the solute from reaching the surface, under aqueous environments. Consequently, the water content of a reversed phase column seems to be a crucial factor in enhancing selectivity while simultaneously reducing residual silanol effects.

REFERENCES

1. J. Cadet, M. Weinfeld, Anal. Chem., **65**, 675A-682A (1993).

2. U. D. Neue, D. J. Phillips, T. H.Walter, M. Capparella, B. Alden, R. P.Fisk, LC-GC, **12**, 468-480 (1994).

3. G. W. Welling, R. van der Zee, S. Welling-Wester, "HPLC of Membrane Proteins", in **HPLC of Biological Macromolecules**, K. M. Gooding, F. E.Regnier, eds., Chromatographic Science Series, J. Cazes, ed., Marcel Dekker, New York, 1990, pp. 373-401.

4. W. S. Hancock, "HPLC in Biotechnology", in **HPLC in Biotechnology**, W. S. Hancock, ed., John Wiley, New York, 1990, pp. 1-19.

5. C. Schoneich, A. F. R. Huhmer, S. R. Rabel, J. F. Stobaugh, S. D. S. Jois, C. K. Larive, T. J. Siahaan, T. C. Squier, D. J. Bigelow, T. D. Williams, Anal. Chem., **67**, 155R-181R (1995).

6. S. K. C. Chang, E. Holm, J. Schwarz, P. Rayas-Duarte, Anal. Chem., **67**, 127R-153R (1995).

7. A. K. D. Liem, R. A. Baumann, A. P. J. M. de Jong, E. G. van der Velde, P. van Zoonen, J. Chromatogr., **624**, 317-339 (1992).

8. R. E. Majors, LC-GC, **12**, 890-898 (1994).

9. L.C. Sander, S.A. Wise, Anal. Chem., **67**, 3284-3292 (1995).

10. J. G. Dorsey, W. T. Cooper, Anal. Chem., **66**, 857A-867A (1994).

11. K. Tani,Y. Suzuki, J. Chromatogr. Sci., **27**, 698-703 (1989).

12. L. C. Sander, S. A. Wise, J. Chromatogr. A, **656**, 335-351 (1993).

13. K. Jinno, T. Ibuki, N. Tanaka, M. Okamoto, J.C. Fetzer, W.R. Biggs, P.R. Griffiths, J. M. Olinger, J. Chromatogr., **461**, 209-227 (1989).

14. R. Gill, D. Osselton, R. M. Smith, T.G. Hurdley, J. Chromatogr., **386**, 65-77 (1987).

15. L. C. Sander, S.A. Wise, Crit. Rev. Anal. Chem., **18**, 299-415 (1987).

16. S.O. Akapo, C.F. Simpson, Anal. Proc., **26**, 394-397 (1989).

17. P. Schneider, R. Cloux, K. Foti, E.sz. Kovats, Synthesis, 1027-1031 (1990).

18. J. J. Kirkland, J.W. Henderson, J. Chromatogr. Sci., **32**, 473-480 (1994).

19. R. Zhang, Z. Xie, R. Zhao, X. Li, G. Liu, M. Aguilar, M.T.W. Hearn, Anal. Chem., **63**, 1861-1867 (1991).

20. R. K. Gilpin, M.E. Gangoda, J. Chromatogr. Sci., **28**, 277-281 (1990).

21. J.E. Sandoval, J.J. Pesek, Anal. Chem., **61**, 2067-2075 (1989).

22. M.J. Wirth, H.O. Fatunmbi, Anal. Chem., **64**, 2783-2786 (1992).

23. P. Tundo, P. Venturello, J. Am. Chem. Soc., **101**, 6606-6613 (1979).

24. N. Oi, M. Nagase, Y. Inda, T. Doi, J. Chromatogr., **259**, 487-493 (1983).

25.A. Nomura, J. Yamada, K. Tsunoda, Anal. Sci., **3**, 209-212 (1987).

26. B. Buszewski, J. Schmid, K. Albert, E. Bayer, J. Chromatogr., **552**, 415-427 (1991).

27. Y. Okahata, K. Kimura, K. Ariga, J. Am. Chem. Soc., **111**, 9190-9194 (1989).

28. G. Boven, R. Folkersma, G. Challa, A.J. Schouten, Polymer Commun., **32**, 50-53 (1991).

29. S. Yamamura, T. Tamaki, T. Seki, M. Sakuragi, Y. Kawanishi, K. Ichmura, Chem. Lett., 543-546 (1992).

30. C. Pidgeon, U. V. Venkataram, Anal. Biochem., **176**, 36-45 (1989).

31. K. M. R. Kallury, M. Cheung, V. Ghaemmaghami, U. J. Krull, M. Thompson, Colloids Surfaces, **63**, 1-9 (1992).

32. T. Ihara, Y. Sugimoto, M. Asada, T. Nakagama, T. Hobo, J. Chromatogr., **694**, 49-56 (1995).

33. S. Nagae, T. Miyamoto, Y. Inaki, K. Takemoto, Polymer J., **21**, 19-33 (1989).

34. W. H. Pirkle, T. C. Pochapsky, Chem. Rev., **89**, 347-362 (1989).

35. C. E. Kibbey, M. E. Meyerhoff, J. Chromatogr., **641**, 49-55 (1993); Anal. Chem., **65**, 2189-2196 (1993).

36. J. E. O'Gara, B. A. Alden, T. H. Walter, J. S. Petersen, C. L. Niederlander, U. D. Neue, Anal. Chem., **67**, 3809-3813.

37. B. Buszewski, M. Jaroniec, R. K. Gilpin, J. Chromatogr., **673**, 11-19 (1994).

38. M. Alvinerie, J. F. Sutra, C. Eeckhoutte, P. Galtier, G. A. E. van't Klooster, A. S. J. P. A. M. van Miert, J. Chromatogr., **612**, 115-121 (1993).

39. R. J. M. Vervoort, M. W. J. Derksen, F. A. Maris, J. Chromatogr., **678**, 1-15 (1994).

40. D. Korakas, K. Valko, J. Liquid Chromatogr., **17**, 3571-3584 (1994).

41. J. Paesen, P. Claeys, E. Roets, J. Hoogmartens, J. Chromatogr., **630**, 117-122 (1993).

42. E. F. Vansant, P. Van Der Voort, K. C. Vrancken, "**Characterization and Chemical Modification of the Silica Surface**", Elsevier, Amsterdam (1995), pp. 489-510.

43. D. Amati, E. Kovats, Langmuir, **3**, 687-695 (1987).

44. M. L. Miller, R. W. Linton, S. G. Bush, J. W. Jorgenson, Anal. Chem., **56**, 2204-2210 (1984).

45. K. M. R.Kallury, M. Thompson, C. P. Tripp, M. L. Hair, Langmuir, **8**, 947-954 (1992).

46. V. A. Brown, D. A. Barrett, P. N. Shaw, M. C. Davies, H. J. Ritchie, P. Ross, A. J. Paul, J. F. Watts, Surface Interface Anal., **21**, 262-272 (1994).

47. B. Buszewski, P. Kasturi, R. K. Gilpin, M. E. Gangoda, M. Jaroniec, Chromatographia, **39**, 155-161 (1994).

48. K. M. R. Kallury, P. M. Macdonald, M. Thompson, Langmuir, **10**, 492-499 (1994).

49. K. M. R. Kallury, M. Thompson, C. P. Tripp, M. L. Hair, Langmuir, **8**, 947-954 (1992).

50. K. Albert, E. Bayer, J. Chromatogr., **544**, 345-370 (1991).

51. G. S. Caravajal, D. E. Leydon, G. R. Quinting, G. E. Maciel, Anal. Chem., **60**, 1776-1786 (1988).

52. H. Saint-Martin, I. Ortega-Blake, "The microscopic structure and dynamics of water at a surface", in "**Enzymes in Reverse Micelles Containing Phospholipids**", A. Darszon, L. Shoshani, eds., CRC Press, Boca Raton, 1992, pp. 35-65.

53. J. Wang, Z. Lu, Anal. Chem., **62**, 826-829 (1990).

54. D. E. Martire, R. E. Boem, J. Phys. Chem., **87**, 1045-1062 (1983).

55. K. A. Dill, J. Phys. Chem., **91**, 1980-1988 (1987).

56. Y. Men, D. B. Marshall, Anal. Chem., **62**, 2606-2611(1990).

57. M. Jaroniec, J. Chromatogr. A, **722**, 19-24 (1996).

58. B. Buszewski, M. Jaroniec, R. K. Gilpin, J. Chromatogr. A, **668**, 293-299 (1994).

59. P. Kasturi, B. Buszewski, M. Jaroniec, R. K. Gilpin, J. Chromatogr. A, **659**, 261-265 (1994).

60. M. Jaroniec, J. Chromatogr. A, **656**, 37-50 (1993).

61. M. Jaroniec, S. Lin, R. K. Gilpin, Chromatographia, **32**, 13-17 (1991).

62. R. K. Gilpin, M. Jaroniec, S. Lin, Anal. Chem., **63**, 2849-2852 (1991); **62**, 2092-2098 (1990).

63. M. Jaroniec, D. E. Martire, J. Chromatogr., **351**, 1-16 (1986); **387**, 55-64 (1987).

Received February 7, 1996
Accepted March 28, 1996
Manuscript 4151